Desalination and Water Treatment
www.deswater.com

doi: 10.5004/dwt.2020.26374

201 (2020) 452–461
October

Treatability of textile industry polyester cloth dyeing wastewater by adsorption and photocatalytic method using $nTiO_2$

N. Pınar Tanatti[a,*], Şeyma Türkyilmaz[b], Füsun Boysan[b], İ. Ayhan Şengil[b]

[a]*Department of Environmental Protection Technologies, Sakarya University of Applied Sciences, Turkey, 54100 Sakarya-Turkey, Tel. +90 264 2957356; Fax: +90 264 2955601; email: ptanatti@sakarya.edu.tr (N. Pınar Tanatti)*
[b]*Department of Environmental Engineering, Engineering Faculty, Sakarya University, 54100 Sakarya-Turkey, Tel. +90 264 2957356; Fax: +90 264 2955601; emails: turkyilmazseyma@gmail.com (Ş. Türkyilmaz), fboysan@sakarya.edu.tr (F. Boysan), asengil@sakarya.edu.tr (İ. Ayhan Şengil)*

Received 14 December 2019; Accepted 21 July 2020

ABSTRACT

Textile industry wastewater includes organic dyes and decomposition products which could have toxic and mutagenic effects on life. The majority of industries in this sector use nonbiodegradable, heat-resistant, light, oxidizing agents and therefore synthetic dyes that are difficult to remove color. In this study, Dianix Yellow Brown CC (0.22%), Dianix Rubine CC (0.79%) and Setapers Blue CE3R (0.015%) containing disperse dye have been used in the production of wastewater from the dyehouse. In this study, textile wastewater has been treated which has applied adsorption and photocatalytic methods by using nano-titanium dioxide ($nTiO_2$). Optimum chemical oxygen demand (COD) and color removal efficiencies have been determined for these two methods. Moreover, under the optimum conditions in the adsorption method, the COD removal efficiency has been obtained as 58.07% and also color removal efficiencies have been obtained as 95.24%, 95.15%, 96.83% for 436, 525 and 620 nm, respectively (pH 2, $nTiO_2$ dose 2.5 g L^{-1} and 30 min reaction time). Therefore, under the optimum conditions in the photocatalytic method the COD removal efficiency has been obtained as 57.59% and also color removal efficiencies have been obtained as 95.24%, 96.31%, 94.71% for 436, 525 and 620 nm, respectively (pH 2, $nTiO_2$ dose 1.5 g L^{-1} and 60 min reaction time). Four different kinetic, that is, first-order kinetic, second-order kinetic, pseudo-first-order, pseudo-second-order, models have been used for the processes adsorption and photocatalytic. The pseudo-second-order kinetic model has been found to be the most suitable model for both processes. As a result, regression coefficients (R^2) has been obtained for adsorption as 1 and for photocatalytic as 0.9999 and reaction rate constants (k) have been obtained for adsorption as 6.9×10^{-4} L mg^{-1} min^{-1} and for photocatalytic as 2.2×10^{-3} L mg^{-1} min^{-1}.

Keywords: Textile wastewater, adsorption, photocatalytic, Nano-titanium dioxide

1. Introduction

Water pollution caused by industrial wastewater (especially the large discharges and complex composition of textile wastewater) and other polluting factors reveals the crisis of freshwater shortage, appeared as one of the most serious global problems that threaten human existence [1].

The available water resources for human activities represent an extremely small proportion of global water reserves (approximately 0.03%) while industrial activity is increasing as a result of the world population growth [2]. Due to the intensive water and chemical usage of the textile industry is one of the most important sectors that constituting industrial pollution in waters [3].

* Corresponding author.

Presented at the 1st International Conference on Environment, Technology and Management (ICETEM), 27–29 June 2019, Nigde, Turkey

Textile industry wastewater contains acids, alkalies, dispersants, synthetic dyes, pigments, biocides, oils, heavy metals, starch, salts, surfactants, nutrients and organic compounds [4,5]. On the other hand, as contamination parameters, textile wastewaters included high values of suspended solids, chemical oxygen demand (COD), biological oxygen demand (BOD), acidity, alkalinity and other dissolved substances [6].

60% of the dyestuffs used in the textile industry are reactive dyestuffs due to their advantages such as bright colors, stability during the washing process and easy application [7,8]. Textile wastewater contains organic dyes and their decomposition products that may have toxic and/or mutagenic effects [8]. The majority of dyes used in this sector are synthetic dyes that non-biodegradable, heat resistant, and contains oxidizing agents, therefore difficult to remove from wastewater [9].

Reactive and azo dyes are mixed with water by washing processes for dyeing textile products. Approximately 10%–20% of these dyes contain harmful substances to human health and the environment [10]. The dye house wastewaters generally contain about 10–50 mg L^{-1} dye and such concentrations are high enough to provide a significant coloration of the receiving water bodies [11].

Physical, chemical and particular biological treatment methods are widely used in the treatment of textile wastewater [12]. However, these chemical and physical methods are nonefficient for reactive and azo dyestuffs because of the secondary waste problems and complexity of their composition. And also, included organic matters are nonbiodegradable and toxic, for biologic treatment methods [4,5,13,14]. Therefore, advanced methods such as adsorption and chemical/electrochemical processes are required to treat wastewater [9]. Coagulation [15], advanced oxidation processes [16–19], adsorption [2,20,21] and combine processes such as electrocoagulation-ozone [22], activated carbon-$FeCl_3$ [23], permanganate-ozone [24] studies have gained importance for textile wastewater treatment. Interest in wastewater treatment research has focused on advanced oxidation processes, an alternative treatment method for the last two decades [13].

In this study, textile dyeing wastewater containing Dianix Yellow Brown CC (0.22%), Dianix Rubine CC (0.79%), and Setapers Blue CE3R (0.015%) dyes have been used. There are no studies in the literature about textile wastewater containing these dyes mixture. It was aimed to treat wastewater by using adsorption and photocatalytic methods using nanotitanium dioxide ($nTiO_2$). Optimum COD and color removal efficiencies have been determined for these two methods.

2. Materials and methods

2.1. Characteristic of textile wastewater

The textile wastewater used in this study was obtained from the textile factory of Sakarya (Turkey). Wastewater has been taken from the washing tank. The textile wastewater used in the experiments is very dirty and contains suspended solids, high COD and BOD, acidity, alkalinity and other dissolved substances. The textile wastewater has a red color and, consisted of disperse dyes (Dianix Yellow Brown CC (0.22%), Dianix Rubine CC (0.79%), and Setapers Blue CE3R (0.015%)). The dyes have classified as azo disperse dyes and included chemicals are N-[5-(diethylamino)-2-[(3,5-dinitro-2-thienyl)azo]phenyl]acetamide (CAS number: 58979-46-7, EC number: 261-540-2). The chemical structure is given in Fig. 1 [20]. λ_{max} values at Dianix Yellow Brown CC, Dianix Rubine CC, and Setapers Blue CE3R are 450, 530 and 620 nm, respectively. And also, the composition of the wastewater is shown in Table 1.

2.2. Analysis methods and chemical

The color analysis has been performed according to EN ISO 7887 B [25] and, measured with Shimadzu UV/Vis 1700 brand spectrophotometer using 50 mm optical quartz cuvettes. The limit values according to European norms are given in Table 3. The COD analysis has been performed according to SM 5220 D [26]. The surface morphology of the films morphologies was examined by scanning electron microscopy (SEM). $nTiO_2$ is 21 nm in diameter and the SEM image for $nTiO_2$ is given Fig. 2. The surface area of the $nTiO_2$ is determined by the Brunauer–Emmett–Teller (BET) assay. The BET analysis report is given in Table 3.

2.3. Photocatalytic treatment

Semiconductor materials and lightly are used to remove organic pollutants. Titanium dioxide (TiO_2) is widely used because of its abundant availability, cost-effectiveness, non-toxicity, high excitation binding energy, and excellent properties such as photocatalytic active crystal phases [27]. Commercially available TiO_2 in various crystal forms and particle properties is photochemical stable. Photocatalytic

Fig. 1. Structure of N-[5-(diethylamino)-2-[(3,5-dinitro-2-thienyl) azo]phenyl]acetamide.

Table 1
Characteristics of textile wastewater

Parameter	Value
pH	4–4.5
COD (mg L^{-1})	1,025.44
Color (m^{-1})	46.2 (436 nm)
	43.3 (525 nm)
	18.9 (620 nm)

Table 2
European norm color limit values

436 nm	525 nm	620 nm
7 m^{-1}	5 m^{-1}	3 m^{-1}

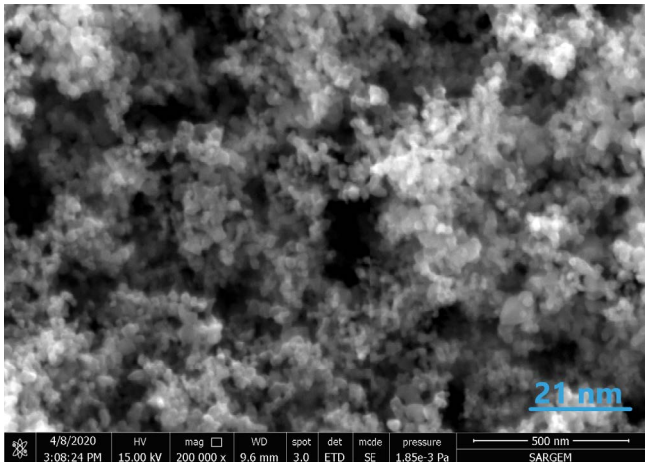

Fig. 2. SEM image for $nTiO_2$.

Table 3
BET analysis report of $nTiO_2$

Parameter	Value
Single point surface area (m^2 g^{-1})	47.4130
BET surface area (m^2 g^{-1})	44.8488
Single point adsorption total pore volume (cm^2 g^{-1})	0.1571
Adsorption average pore width (by BET) (nm)	14.0123

treatment can greatly reduce the organic pollution load of textile wastewater and similar wastewater [28].

The photocatalytic reaction is a chemical reaction based on the action of free radicals by the interaction of molecules of photons in solution at an appropriate energy level to remove undesirable contaminants [29]. Oxidation of colored substances using catalyst-assisted photon energy; has a remarkable position in the growth processes. Heterogeneous photocatalysis; paint is an advanced oxidation process sufficient to provide oxidation of organics and inorganics containing [30].

In summary and in simplistic form, the relevant reactions at the semiconductor surface (TiO_2) causing the degradation of dyes can be expressed as follows [19]:

$$TiO_2 + h\upsilon(UV) \rightarrow TiO_2\ (e^-_{CB} + h^+_{VB}) \quad (1)$$

$$TiO_2(h^+_{VB}) + H_2O \rightarrow TiO_2 + {}^{\bullet}OH_{ads} + H^+ \quad (2)$$

$$TiO_2(h^+_{VB}) + OH^- \rightarrow TiO_2 + {}^{\bullet}OH_{ads} \quad (3)$$

$$TiO_2(e^-_{CB}) + O_{2(ads)} \rightarrow TiO_2 + O_2^{\bullet-} \quad (4)$$

$$O_2^{\bullet-} + H^+ \rightarrow HO_2^{\bullet-} \quad (5)$$

$$\text{Dye} + {}^{\bullet}OH \rightarrow \text{degradation products} \quad (6)$$

$$\text{Dye} + h^+_{VB} \rightarrow \text{oxidation products} \quad (7)$$

$$\text{Dye} + e^-_{CB} \rightarrow \text{reduction products} \quad (8)$$

There are 6 UV lamps in the reactor and the lamps have 254 nm wavelength. Each lamp has a 6-watt power and the reactor has a total of 36 watts energy. TiO_2 (21 nm) was used as the photocatalyst. The reactor vessel is a quartz vessel with a volume of 200 mL.

2.4. Adsorption treatment

Adsorption is one of the most simple, reliable, economical and efficient technologies among traditional wastewater treatment technologies [27].

The adsorption method is an effective method for removing contaminants such as color which are difficult to remove by conventional methods. Adsorption is an economically viable method, apart from the initial investment cost. The adsorption process is influenced by many physicochemical factors such as surface area, particle size, temperature, pH, and contact time of the dye/sorbent interaction [31].

Natural adsorbents such as corn cob, rice husk, wood, wood clippings are involved in paint removal applications, but their effectiveness is higher on basic paints than acid paints. Since the usage of basic dyes is not very common in the textile industry, usage applications are limited [31].

Experiments have been carried out using 250 mL flasks and an adjustable stirrer in the adsorption system.

3. Results and discussion

3.1. Effect of pH

pH is an effective parameter in photocatalytic and adsorption methods. It has a significant effect on the retention of dyes. The pH value of the solution in photocatalytic reactions may affect the electrostatic charge on the surface of $nTiO_2$. Therefore, pH is a factor determining the photocatalyst surface charge density and thus the photocatalytic oxidation efficiency. In the case of purification by adsorption, the adsorption of other ions is influenced by the solution pH, since hydronium and hydroxyl ions are strongly adsorbed. Besides the degree of ionization of acidic or basic compounds affects the adsorption.

In this study, the effect of pH on color and COD removal efficiencies has been investigated in the textile industry wastewater. In this study, 2,3,5,7,9 as pH are used for both processes considering 10 g L^{-1} as $nTiO_2$ and 60 min as reaction time. COD removal efficiencies in treatment by photocatalytic and adsorption methods have been given in Fig. 3 and color removal efficiencies have been given in Fig. 4.

COD removal efficiencies which are shown in Fig. 3 in the photocatalytic process is higher than the adsorption process. Removal efficiency is high at low pH in the adsorption method. Moreover, the COD removal efficiencies have appeared to decrease after pH 7 in the photocatalytic

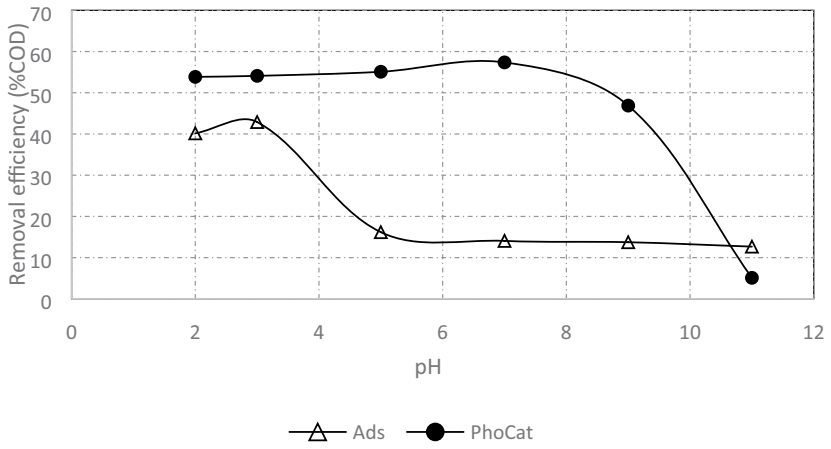

Fig. 3. Effect of pH on COD removal efficiency by adsorption and photocatalytic methods ($C_{0\text{–COD}}$ = 1,025 mg L^{-1}; $nTiO_2$ = 10 g L^{-1}; t = 60 min; mixing speed = 150 rpm).

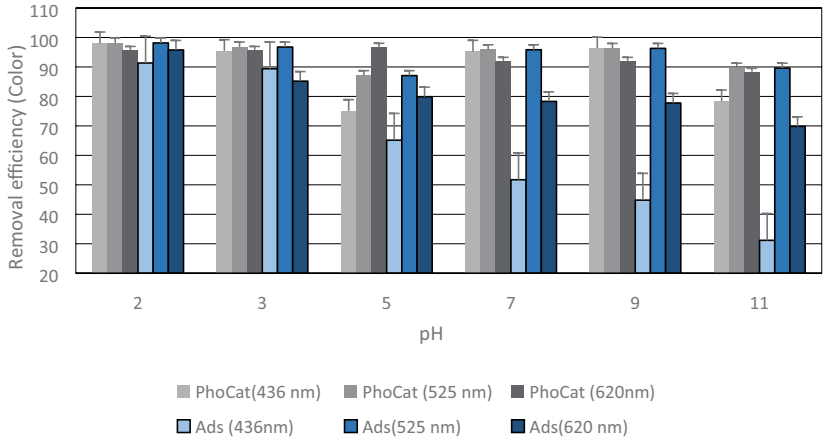

Fig. 4. Effect of pH on color removal efficiency by adsorption and photocatalytic methods ($C_{0\text{–436 nm}}$ = 46.2 m^{-1}; $C_{0\text{–525 nm}}$ = 43.3 m^{-1}; $C_{0\text{–620 nm}}$ = 18.9 m^{-1}; $nTiO_2$ = 10 g L^{-1}; t = 60 min; mixing speed = 150 rpm).

method. Fig. 4 show that color removal efficiencies have been high for both processes at low pH. Color removal efficiency decreases from 98% in pH 2 to 88% in pH 11 in the photocatalytic treatment method. While pH 2 has 94% removal efficiency, pH 11 decreases to 35% in the adsorption treatment method. Removal efficiency decreases around 10% with a pH increase in photocatalytic treatment at different pH. However, the removal efficiency in the adsorption method tends to decrease considerably. The pH value of the textile wastewater used in the study is 4. pH 2 optimum results have been obtained in the photocatalytic and adsorption method. Therefore, since the pH value of the wastewater used in the study is low, it is possible to work with pH 2 in commercial applications. COD removal efficiencies have been achieved 53.84% in the photocatalytic method and 40.15% in the adsorption method for pH 2. Color removal efficiencies have been obtained to be 91.34%, 94.92%, 95.77% for adsorption and 98.05%, 98.15%, and 95.77% for photocatalytic, respectively at 436, 525 and 620 nm at pH 2.

Zeta potential analyses were measured with the zeta sizer brand Nano-ZS model device. The zeta potential values of $nTiO_2$ as a function of pH are given in Table 4. Any change in solution pH will reposition the potentials of photocatalytic reactions and affect the surface charge of the TiO_2 particles. It will bring about a change in reaction rate, respectively [19]. The zeta potential of TiO_2 is maximum at low pH. Zeta potential decreases with increasing pH. Especially the zeta potential, which is positive up to pH 6–7, becomes negative after these values. At low pH, the surface charges turn out to positive values after the zero charge point (after pH 6.5) aggregation begins on the surface of the nanoparticles [32]. At more alkaline pH values, particle size starts to increase. And positively charged particles repel each other with the effect of low pH [33].

Depending on the pH, zeta potentials were found as negative at pH 9 and also, in low pH, zeta potential values were achieved as the positive values, in this study.

3.2. Effect of $nTiO_2$ dose

Both processes have been studied for COD and decolorization parameters at 60 min reaction times at pH 2.

$nTiO_2$ dose between 1 and 20 g L^{-1} have experienced in the photocatalytic and the adsorption methods.

COD removal efficiency has been found 16.96% at 1 g L^{-1} $nTiO_2$ dose and 59.99% at 20 g L^{-1} $nTiO_2$ dose in the adsorption method (Fig. 5). Besides that for the photocatalytic method has been achieved by 44.21% in 1 g L^{-1} $nTiO_2$ dose, and 61.05% in 20 g L^{-1} $nTiO_2$ dose. As seen in Fig. 5 COD values increased up with the dose 2.5 g L^{-1} $nTiO_2$ in the adsorption method and after that, no significant removal has been observed. Furthermore, in the photocatalytic method after 1.5 g L^{-1} $nTiO_2$ dose COD removal rates were not increased as indicated in Fig. 5. COD removal has been acquired to 53.19% at 2.5 g L^{-1} $nTiO_2$ dose in the adsorption method and 50.56% at 1.5 g L^{-1} $nTiO_2$ dose in the photocatalytic method.

Table 4
Zeta potentials of $nTiO_2$ depending on the pH

pH	Zeta potential (mV)
2	2.61
3	1.388
5	0.691
7	0.218
9	–3.33

While the dose of nano-titanium dioxide with the lowest color removal was 1 g L^{-1} in both processes, it was observed that removal efficiency increased very slowly, above this value of nano-titanium dioxide. As specified in Fig. 6, the color measurements have been pursued at 435, 525, and 620 in order. Based on the wavelength (435nm, 525, and 620 nm) color removal efficiencies were obtained as 93.94%, 94.46%, and 93.65% respectively for the adsorption method at the dose of 2.5 g L^{-1} $nTiO_2$ in the photocatalytic method with 1.5 g L^{-1} $nTiO_2$ dose, these values have alternated at 95.89%, 97.23%, and 95.24%.

Although both methods have studied at the same pH, the efficiency of the adsorption method is obtained by

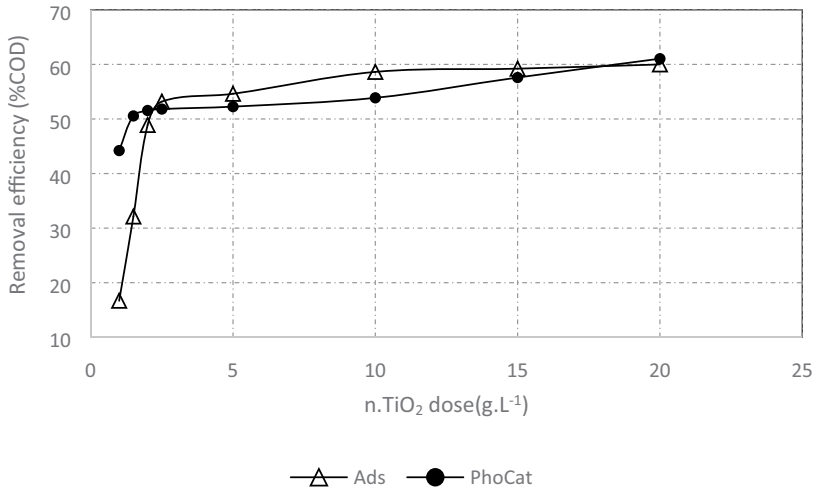

Fig. 5. Effect of $nTiO_2$ dose on COD removal efficiency by adsorption and photocatalytic methods ($C_{0\text{–COD}}$ = 1,025 mg L^{-1}; pH = 2; t = 60 min; mixing speed = 150 rpm).

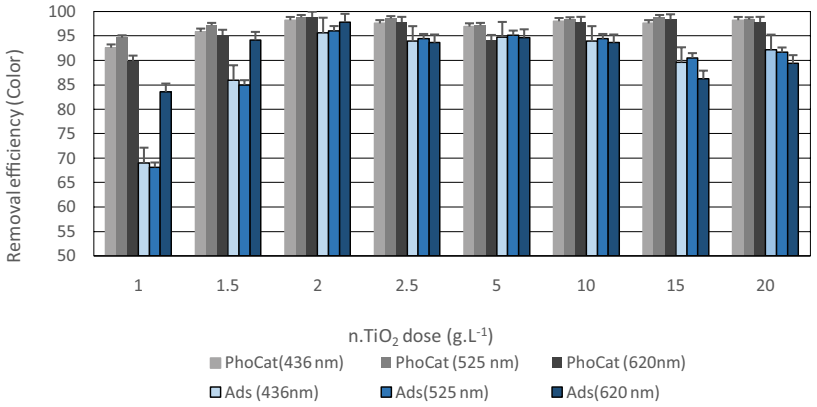

Fig. 6. Effect of $nTiO_2$ dose on color removal efficiency by adsorption and photocatalytic methods ($C_{0\text{–}436\ nm}$ = 46.2 m^{-1}; $C_{0\text{–}525\ nm}$ = 43.3 m^{-1}; $C_{0\text{–}620\ nm}$ = 18.9 m^{-1}; pH = 2; t = 60 min; mixing speed = 150 rpm).

using a lower TiO_2 dose in the photocatalytic method since TiO_2 has high zeta potential in the photocatalytic method at low pH.

3.3. Effect of the reaction time

The reaction time of COD and color removal have been studied at pH 2 for both processes. Although the TiO_2 dose was 2.5 g L^{-1} in the adsorption method, it was 1.5 g L^{-1} in the photocatalytic method. In Figs. 7 and 8 have been given COD and color removal efficiencies.

Fig. 7 shows that there is a very slow rise in COD removal performances up to 60 min for both processes. Also, after 60 min, the change in removal efficiency change has happened too little. While COD removal efficiency was found of 53.55% for 15 min and 59.87% for 240 min in the adsorption process, efficiency was found of 51.77% for 15 min and 60.80% for 240 min in the photocatalytic process. COD removal efficiencies for 60 min have been obtained as 58.07% and 57.59% in adsorption and photocatalytic methods, respectively.

Color removal efficiencies were found upon 90% in both processes. The color removal efficiencies were shown in Fig. 8 as 95.24%, 95.15%, and 96.83% for 436, 525 and 620 nm for adsorption method at 60 min reaction time. The removal efficiencies for the same wavelengths have been obtained 95.24%, 96.31%, and 94.71% in the photocatalytic method, respectively.

3.4. Kinetic analysis of COD and color removal efficiencies

Adsorption and photocatalytic treatment efficiencies were examined in four different kinetics. The equations of the studied kinetic models are given.

$$\ln\frac{C_0}{C} = k \cdot t \quad \text{[34] (9)}$$

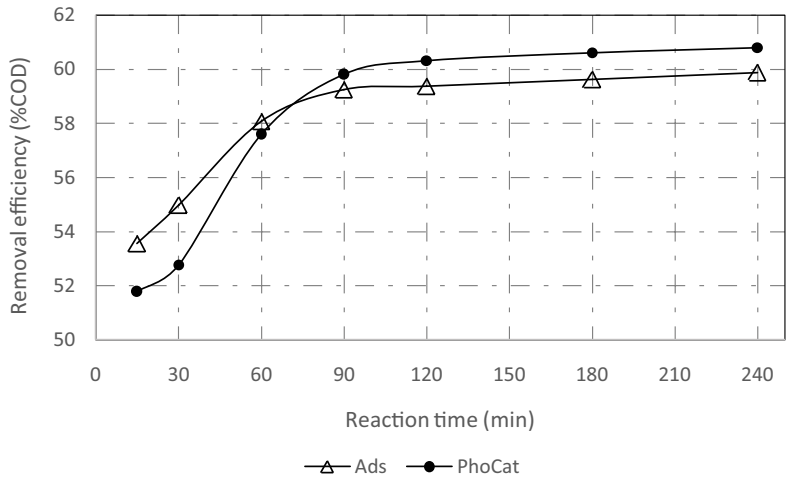

Fig. 7. Effect of reaction time on COD removal efficiency by adsorption and photocatalytic methods ($C_{0\text{–COD}}$ = 1,025 mg L^{-1}; pH = 2; $nTiO_{2(ads)}$ = 2.5 g L^{-1}; $nTiO_{2(ads)}$ = 1.5 g L^{-1}; mixing speed = 150 rpm).

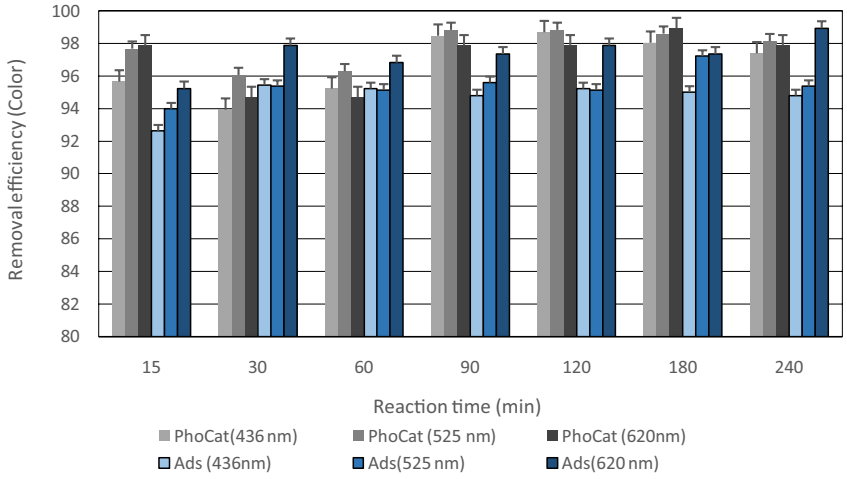

Fig. 8. Effect of reaction time on color removal efficiency by adsorption and photocatalytic methods ($C_{0\text{–}436\,nm}$ = 46.2 m^{-1}; $C_{0\text{–}525\,nm}$ = 43.3 m^{-1}; $C_{0\text{–}620\,nm}$ = 18.9 m^{-1}; pH = 2; $nTiO_{2(ads)}$ = 2.5 g L^{-1}; $nTiO_{2(ads)}$ = 1.5 g L^{-1}; mixing speed = 150 rpm).

$$\frac{1}{C}-\frac{1}{C_0}=k\cdot t \quad \text{[35] (10)}$$

$$\ln\left[C_e-C_{(t)}\right]=\ln C_e-k\cdot t \quad \text{[36] (11)}$$

$$\frac{t}{C}=\frac{1}{k\cdot C_e^2}+\frac{1}{C_e}\cdot t \quad \text{[37] (12)}$$

Reaction rate constants and regression coefficients (R^2) according to first-order, second-order, pseudo-first-order and pseudo-second-order kinetic models are given in the tables.

Table 5 shows that the reaction rate (k) and regression coefficient (R^2) values of the kinetic models inspected on COD removal efficiencies for both methods. The pseudo-second-order model is significant among the kinetic models. The regression coefficient and k value of the second-order model for the adsorption method were 1 and 0.00069 L dk^{-1} mg^{-1}, respectively. In addition, for the photocatalytic method with the pseudo-second-order equation, R^2 and reaction rate constant (k) has been calculated as 0.9999 and 0.00022 L mg^{-1} min^{-1}.

By using the kinetic models along with the calculated k, and R^2 values are listed in Table 6, the color removal efficiencies have been determined, for the adsorption method. The pseudo-second-order model is significant among the kinetic models as well as its were significant COD kinetic model. According to the pseudo-second-order equation, R^2 and k values were calculated for three different wavelengths. At the adsorption method, according to the pseudo-second-order equation, R^2 and k values were calculated for three different wavelengths. The results can be summarized as, R^2 = 1 and k = 0.00069 L mg^{-1} min^{-1}.for 432 nm, R^2 = 0.9998, k = 0.08 L mg^{-1} min^{-1} for 525 nm, and R^2 = 0.9999, k = 0.05863 L mg^{-1} min^{-1} for 620 nm.

The k and R^2 values of the kinetic models investigated on the color removal efficiencies have been given in Table 7 for the photocatalytic method. The pseudo-second-order model is significant among the kinetic models. R^2 values calculated by pseudo-second-order equations are determined as 0.9998, 0.9999 and 0.9998 for 436, 525 and 620 respectively, while the k values are figured out, as 0.03971, 0.05952 and 0.05483 L mg^{-1} min^{-1} in order.

The theoretically calculated COD and color values, by using the reaction rate constant and equilibrium concentration were acquired from the pseudo-second-order kinetic. The comparison of the theoretical and the experimental results have shown in Figs. 9–11.

As shown in Fig. 9, theoretical COD and experimental COD results were both decreased similarly depending on the reaction time, for two methods. Theoretical color

Table 5
k and R^2 values for COD removal efficiency

Kinetic model	Adsorption		Photocatalytic	
	R^2	k	R^2	k
First-order[a]	0.6617	0.0006	0.3559	0.0006
Second-order[b]	0.6716	0.000001	0.3442	0.000001
Pseudo-first-order[c]	0.9303	0.0207	0.9459	0.0276
Pseudo-second-order[d]	1	0.00069	0.9999	0.00222

[a]k unit: min^{-1}; [b]k unit: L mg^{-1} min^{-1}; [c]k unit: mg L^{-1} min^{-1}; [d]k unit: L mg^{-1} min^{-1}

Table 6
k and R^2 values for color removal efficiencies in adsorption method

Kinetic model	436 nm		525 nm		620 nm	
	R^2	k	R^2	k	R^2	k
First-order[a]	0.0768	0.005	0.2955	0.0016	0.5787	0.0043
Second-order[b]	0.5931	0.0117	0.5016	0.0019	0.5931	0.0117
Pseudo-first-order[c]	0.0878	0.00346	0.1989	0.00138	0.1587	0.00299
Pseudo-second-order[d]	1	0.5198	0.9998	0.08	0.9999	0.05863

[a]k unit: min^{-1}; [b]k unit: L mg^{-1} min^{-1}; [c]k unit: mg L^{-1} min^{-1}; [d]k unit: L mg^{-1} min^{-1}

Table 7
k and R^2 values for color removal efficiencies in photocatalytic method

Kinetic model	436 nm		525 nm		620 nm	
	R^2	k	R^2	k	R^2	k
First-order[a]	0.2969	0.004	0.3317	0.004	0.2621	0.0032
Second-order[b]	0.3147	0.0092	0.3062	0.0022	0.3147	0.0092
Pseudo-first-order[c]	0.2094	0.00599	0.5088	0.00737	0.2021	0.00392
Pseudo-second-order[d]	0.9998	0.03971	0.9999	0.05952	0.9998	0.05483

[a]k unit: min^{-1}; [b]k unit: L mg^{-1} min^{-1}; [c]k unit: mg L^{-1} min^{-1}; [d]k unit: L mg^{-1} min^{-1}

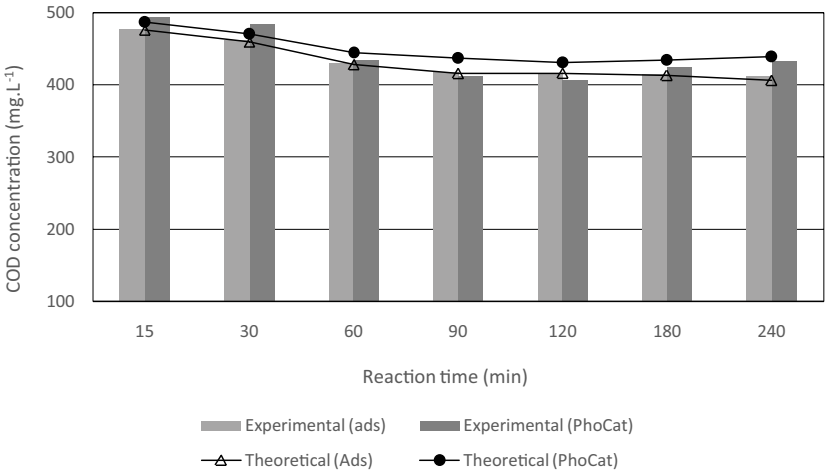

Fig. 9. Change of the theoretical COD value and experimental COD value according to the reaction time calculated according to the pseudo-second-order kinetic model.

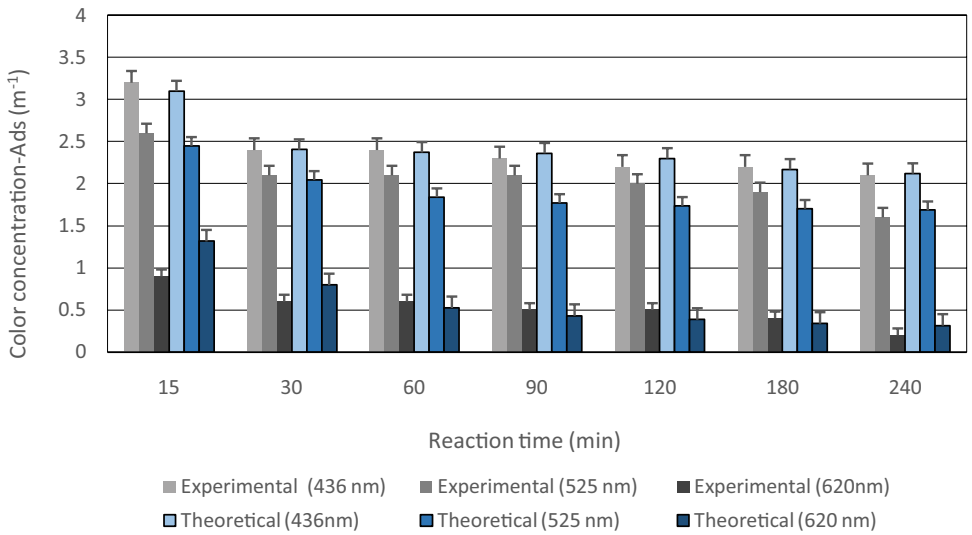

Fig. 10. Change of the theoretical color value and experimental color value according to the reaction time calculated as to the pseudo-second-order kinetic model in the adsorption method.

concentration results calculated with the pseudo-second-order kinetic model, and experimental results are presented in Figs. 10–11 for the adsorption method and the photocatalytic method. Figs. 10 and 11 show that the color concentrations decrease as the reaction time increases. When the kinetic model was examined, significant results have obtained depending on 3 different wavelengths. In particular, at 420 nm wavelength, the theoretical results have been overlapping one to one with the experimental results.

4. Conclusions

Textile wastewater has shown different characteristics due to the dyestuffs used in production. In this study, textile dyeing wastewater from the dyehouse containing Dianix Yellow Brown CC (0.22%), Dianix Rubine CC (0.79%) and Setapers Blue CE3R (0.015%) dyes were used. There are no studies in the literature about textile wastewater containing these dyes. It was aimed to treat wastewater by using adsorption and photocatalytic methods using nano-titanium dioxide ($nTiO_2$). Optimum COD and color removal efficiencies have been determined for these two methods.

Optimum textile wastewater treatment parameters were determined as pH 2, 30 min reaction time, 2.5 g L^{-1} $nTiO_2$ dose and 25°C temperature for the adsorption process. And also for the photocatalytic treatment process, optimum parameters were obtained as pH 2, 60 min reaction time and 1.5 g L^{-1} $nTiO_2$ dose. While under optimum conditions for COD removal have been supplied 50% efficiency for the photocatalytic treatment and 55% efficiency has been reached by adsorption treatment. Color removal efficiencies were found as 95% and 93% with the usage of optimum parameters for photocatalytic treatment and adsorption treatment, respectively.

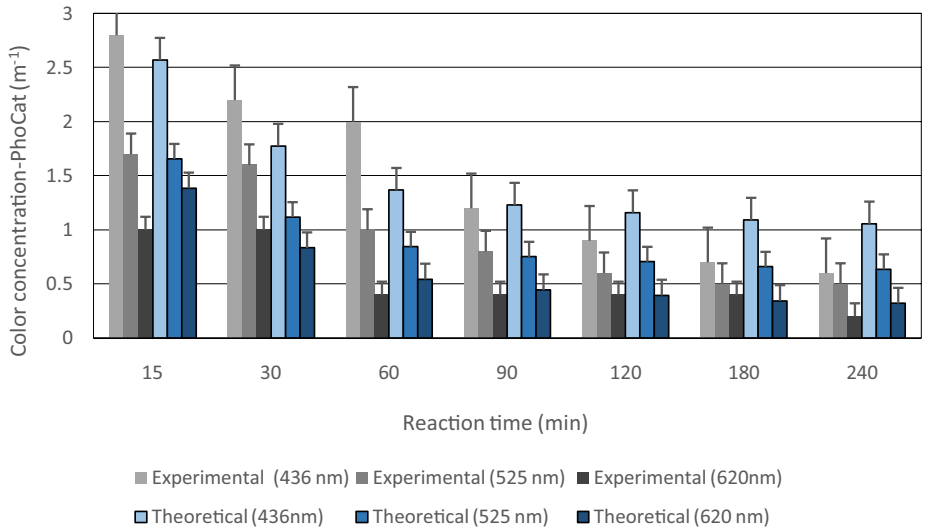

Fig. 11. Change of the theoretical color value and experimental color value according to the reaction time calculated as to the pseudo-second-order kinetic model in the photocatalytic method.

References

[1] C. Liu, Y.Q. Guo, X.J. Wei, C. Wang, M.C. Qu, D.W. Schubert, C.H. Zhang, An outstanding antichlorine and antibacterial membrane with quaternary ammonium salts of alkenes via *in situ* polymerization for textile wastewater treatment, Chem. Eng. J., 384 (2020) 123306.

[2] T.W. Leal, L.A. Lourenço, A.S. Scheibe, U. Guelli, S.M.A. de Souza, A.A.U. de Souza, Textile wastewater treatment using low-cost adsorbent aiming the water reuse in dyeing process, J. Environ. Chem. Eng., 6 (2018) 2705–2712.

[3] N. Takahashi, T. Kumagai, Removal of dissolved organic carbon and color from dyeing wastewater by pre-ozonation and subsequent biological treatment, Ozone Sci. Eng., 28 (2006) 199–205.

[4] J. Blanco, F. Torrades, M. de la Varga, J. García-Montaño, Fenton and biological-Fenton coupled processes for textile wastewater treatment and reuse, Desalination, 286 (2012) 394–399.

[5] C.R. Holkar, A.J. Jadhav, D.V. Pinjari, N.M. Mahamuni, A.B. Pandit, A critical review on textile wastewater treatments: possible approaches, J. Environ. Manage., 182 (2016) 351–366.

[6] A. Birgül, Use of Advanced Oxidation Processes in Textile Industry Wastewater Treatment, Master Thesis, Uludağ Üniversity Institute of Science, Bursa-Turkey, 2006, pp. 1–124.

[7] X.Y. Yang, B. Al-Duri, Application of branched pore diffusion model in the adsorption of reactive dyes on activated carbon, Chem. Eng. J., 83 (2001) 15–23.

[8] O. Türgay, G. Ersöz, Ş. Atalaya, J. Forss, U. Welander, The treatment of azo dyes found in textile industry wastewater by anaerobic biological method and chemical oxidation, Sep. Purif. Technol., 79 (2011) 26–33.

[9] A. Sharma, Z. Syed, U. Brighu, A.B. Gupta, C. Ram, Adsorption of textile wastewater on alkali-activated sand, J. Cleaner Prod., 220 (2019) 23–32.

[10] M.R. Al-Mamun, S. Kader, M.S. Islam, M.Z.H. Khan, Photocatalytic activity improvement and application of UV-TiO_2 photocatalysis in textile wastewater treatment: a review, J. Environ. Chem. Eng., 7 (2019) 1032–1048.

[11] A. Alinsafi, F. Evenou, E.M. Abdulkarim, M.N. Pons, O. Zahraa, A. Benhammou, A. Yaacoubi, A. Nejmeddine, Treatment of textile industry wastewater by supported photocatalysis, Dyes Pigm., 74 (2007) 439–445.

[12] S. Chakraborty, S. De, J.K. Basu, S. DasGupta, Treatment of a textile effluent: application of a combination method involving adsorption and nanofiltration, Desalination, 174 (2005) 73–85.

[13] S.K. Kansal, M. Singh, D. Sud, Studies on photodegradation of two commercial dyes in aqueous phase using different photocatalysts, J. Hazard. Mater., 141 (2007) 581–590.

[14] K. Paździor, J. Wrębiak, A. Klepacz-Smółka, M. Gmurek, L. Bilińska, L. Kos, J. Sójka-Ledakowicz, S. Ledakowicz, Influence of ozonation and biodegradation on toxicity of industrial textile wastewater, J. Environ. Manage., 195 (2017) 166–173.

[15] J. Dotto, M.R. Fagundes-Klen, Performance of different coagulants in the coagulation/flocculation process of textile wastewater, J. Cleaner Prod., 208 (2019) 656–665.

[16] A. Buthiyappan, A.A.A. Raman, Energy intensified integrated advanced oxidation technology for the treatment of recalcitrant industrial wastewater, J. Cleaner Prod., 206 (2019) 1025–1040.

[17] S.G. Cetinkaya, M.H. Morcali, S. Akarsu, C.A. Ziba, M. Dolaz, Comparison of classic Fenton with ultrasound Fenton processes on industrial textile wastewater, Sustainable Environ. Res., 28 (2018) 165–170.

[18] J. Khatri, P.V. Nidheesh, T.S.A. Singh, M.S. Kumar, Advanced oxidation processes based on zero-valent aluminum for treating textile wastewater, Chem. Eng. J., 348 (2018) 67–73.

[19] H.U. Farouk, A.A.A. Raman, W.M.A.W. Daud, TiO_2 catalyst deactivation in textile wastewater treatment: current challenges and future advances, J. Ind. Eng. Chem., 33 (2016) 11–21.

[20] M.J.P. Brito, C.M. Veloso, L.S. Santos, R.C.F. Bonomo, R.C.I. Fontan, Adsorption of the textile dye Dianix® royal blue CC onto carbons obtained from yellow mombin fruit stones and activated with KOH and H_3PO_4: kinetics, adsorption equilibrium and thermodynamic studies, Powder Technol., 339 (2018) 334–343.

[21] S. Wong, N.A.N. Yac'cob, N. Ngadi, O. Hassan, I.M. Inuwa, From pollutant to solution of wastewater pollution: synthesis of activated carbon from textile sludge for dye adsorption, Chin. J. Chem. Eng., 26 (2018) 870–878.

[22] L. Bilińska, K. Blus, M. Gmurek, S. Ledakowicz, Coupling of electrocoagulation and ozone treatment for textile wastewater reuse, Chem. Eng. J., 358 (2019) 992–1001.

[23] Z.H. Xu, Z.H. Sun, Y.W. Zhou, W.F. Chen, T.Q. Zhang, Y.X. Huang, D.F. Zhang, Insights into the pyrolysis behavior and adsorption properties of activated carbon from waste cotton textiles by $FeCl_3$-activation, Colloids Surf., A, 582 (2019) 123934.

[24] J.Y. Liang, X.-A. Ning, J. Sun, J. Song, Y.X. Hong, H. Cai, An integrated permanganate and ozone process for the treatment of textile dyeing wastewater: efficiency and mechanism, J. Cleaner Prod., 204 (2018) 12–19.

[25] BSI Standard Publication, Water Quality-Examination and Determination of Color, European Standards, (ISO 7887:2011).
[26] APHA/AWWA/WEF, Standard Methods for the Examination of Water and Wastewater, 23rd ed., American Public Health Association/American Water Works Association/Water Environment Federation, Washington, D.C., USA, 2017.
[27] T. Fazal, A. Razzaq, F. Javed, A. Hafeez, N. Rashid, U.S. Amjad, M.S.U. Rehman, A. Faisal, F. Rehman, Integrating adsorption and photocatalysis: a cost effective strategy for textile wastewater treatment using hybrid biochar-TiO_2 composite, J. Hazard. Mater., 390 (2020) 12623.
[28] P.A. Parakis, N.P. Xekoukoulotakis, D. Mantzavinos, Treatment of textile dyehouse wastewater by TiO_2 photocatalysis, Water Res., 40 (2006) 1276–1286.
[29] S. Devipriya, S. Yesodharan, Photocatalytic degradation of pesticide contaminants in water, Sol. Energy Mater. Sol. Cells, 86 (2004) 309–348.
[30] M.M. El-Moselhy, Photo-Degradation of Acid Red 44 using Al and Fe Modified Silicates Chemistry Department, Faculty of Science, Al-Azhar University, Nasr City, Cairo, Egypt, 2009.
[31] K.S. Low, C.K. Lee, Quaternized rice husk as sorbent for reactive dyes, Bioresour. Technol., 61 (1997) 121–125.
[32] M.O. Fatehah, H.A. Aziz, S. Stoll, Stability of ZnO nanoparticles in solution, influence of pH, dissolution, aggregation and disaggregation effects, J. Colloid Sci. Biotechnol., 3 (2014) 75–84.
[33] C. Curtis, D. Toghani, B. Wong, E. Nancea, Colloidal stability as a determinant of nanoparticle behavior in the brain, Colloids Surf., B, 170 (2018) 673–682.
[34] S.S. Silva, O. Chiavone-Filho, E.L.B. Neto, E.L. Foletto, Oil removal from produced water by conjugation of flotation and photo-Fenton processes, J. Environ. Manage., 147 (2015) 257–263.
[35] K. Rajeshwar, M.E. Osugi, W. Chanmanee, C.R. Chenthamarakshan, M.V.B. Zanoni, P. Kajitvichyanukul, R. Krishnan-Ayer, Heterogeneous photocatalytic treatment of organic dyes in air and aqueous media, J. Photochem. Photobiol., C, 9 (2008) 171–192.
[36] J.P. Simonin, On the comparison of pseudo-first-order and pseudo-second-order rate laws in the modeling of adsorption kinetics, Chem. Eng. J., 300 (2016) 254–263.
[37] M. Özacar, İ.A. Şengil, Two-stage batch sorber design using second-order kinetic model for the sorption of metal complex dyes onto pine sawdust, Biochem. Eng. J., 21 (2004) 39–45.